Constant Voltage and Frequency Operation of a Two Windings Single Phase Self-Excited Induction Generator

H. H. Hanafy
Electrical Power Engineering Department, Faculty of Engineering, Cairo University, Giza 12613, Egypt
hanafy_hassan@hotmail.com

Heba M. Soufi **Amr A. Saleh** **Magdy B. Eteiba**
Electrical Engineering Department, Faculty of Engineering, Fayoum University, Fayoum 63514, Egypt
hms00@fayoum.edu.eg aae00@fayoum.edu.eg mbe00@fayoum.edu.eg

Abstract: *This paper presents the steady-state and dynamic analysis of a two windings single phase self-excited induction generator (TWSPSEIG) equipped with an excitation capacitor and a compensation capacitor for operation at constant rated load voltage and frequency irrespective the no load or different load conditions. The performance equations at steady-state conditions are obtained by applying loop impedance method via the exact equivalent circuit models of the TWSPSEIG based on the double revolving field theory. Rather than the conventional methods of analysis, to get two non-linear higher order equations keeping the magnetizing reactance and the frequency as unknowns, these equations are rearranged to get two second order equations keeping the values of the excitation capacitor and the compensation capacitor as unknowns for given values of generator parameters, prime mover speed, output frequency and load impedance. The two second order equations are solved using simple iterative method to calculate the optimum values of the two capacitors under the constrains that the load voltage and frequency are constant at rated values. The range of capacitors variations required for maintaining constant rated load voltage and frequency while supplying variable load at variable prime mover speed are calculated. The steady-state results are confirmed by developing a dynamic model of the TWSPSEIG incorporating its nonlinearity behavior and various no-load and load conditions. The dynamic behavior of the TWSPSEIG at different operating conditions proves the capabilities of the proposed configuration and calculations method to maintain both the load voltage and frequency constants.*

Key words: *single phase self-excited induction generator, voltage and frequency control, steady-state and dynamic models.*

Nomenclature

a	:	p.u. frequency.
b	:	p.u. speed.
l_{1A}	:	Auxiliary winding leakage inductance.
l_{1M}	:	Main winding leakage inductance.
l_2	:	Rotor leakage inductance referred to the main winding.
l_{2A}	:	Rotor leakage inductance referred to the auxiliary winding.
l_{mag}	:	Main winding magnetizing inductance.
l_{magA}	:	Auxiliary winding magnetizing inductance.
R_{1M}	:	Main winding resistance.
R_{1A}	:	Auxiliary winding resistance.
R_2	:	Rotor resistance referred to the main winding.
R_{2A}	:	Rotor resistance referred to the auxiliary winding.
t	:	Turns ratio (N_a/N_m).
X_{1M}	:	Main winding reactance.
X_{1A}	:	Auxiliary winding reactance.
X_2	:	The rotor leakage reactance referred to the main winding.
X_{2A}	:	The rotor leakage reactance referred to the auxiliary winding.
X_{mag}	:	Main winding magnetizing reactance.
X_{magA}	:	Auxiliary winding magnetizing reactance.
p	:	The derivative with respect to time.
ω_r	:	The electrical rotor speed.

1. Introduction

The single phase self-excited induction generators (SPSEIGs) are the best choice for supplying small and isolated loads, where grid extension is not possible. The rugged cage rotor construction, low cost, absence of separate exciter, self-protection against fault and stable operation are the main advantages of the SPSEIGs. The self-excitation of the SPSEIGs is similar to that in the 3-phase induction generators, as they are unable to generate their air gap magnetic field. So, in the isolated mode, they must be equipped with terminal capacitors, for supplying their air gap magnetic field in the form of reactive power.

The key factor for voltage building up in SPSEIGs is the selection of the proper excitation capacitance [1-4]. The SPSEIGs can be operated in two different classes which are the single winding SPSEIGs (SWSPSEIG)

and the two windings SPSEIGs (TWSPSEIG). In the single winding class, both the excitation capacitor and load are connected in parallel across the main winding [3, 5]. In the two winding class, a fixed capacitor is connected across the auxiliary winding for the excitation purpose and a compensation capacitor is placed in series/parallel with the load across the main winding [6-7].

Steady-state analysis of SWSPSEIG is always carried out using the double revolving field theory, while that of TWSPSEIG is always carried out using the double revolving field theory combined with the symmetrical components theory. Then the performance equations of the SPSEIG are obtained using nodal admittance or loop impedance methods applied to the SPSEIG circuits. Two nonlinear higher order simultaneous equations are constructed manually by equating the real and imaginary parts of the complex impedance or admittance to zero. These equations have the magnetizing reactance and frequency as two unknowns while their coefficients are functions of the SPSEIG parameters, prime-mover speed, load impedance and the capacitors used according to the configuration of the SPSEIG. The two nonlinear higher order simultaneous equations are then solved by numerical methods such as Newton Raphson method [2], Rosenbrock's method of rotating coordinate [4] and Matlab-fsolve [1,3]. Once the equations are solved the analysis of the SPSEIG performance becomes straight forward. In [8] the author presented an approach which is based on minimizing the impedance equation of the generator to calculate the unknown parameters. The presented approach is easier to implement than other methods of analysis and could be carried out within Matlab software. In [9] the authors developed mathematical models of SPSEIG using graph theory. Graph theory is used since it results in matrix form and the same models can be used for any load and any combination of unknown parameters of the equivalent circuit. Also method using genetic algorithm has been developed.

The major disadvantages of the SPSEIGs are the poor voltage regulation, low output power and efficiency due to the nonlinearity behavior of the SPSEIGs and impact of the backward rotating field. There is wide literature on improving the voltage regulation and output power. To improve the voltage regulation of the SPSEIG different capacitor topologies are introduced such as capacitor connected in series; shunt, long shunt, and short shunt connection with load [10-13]. In [14] a genetic algorithm has been used to optimize the voltage regulation through the selection of the optimum capacitors values for different SPSEIG topologies. It was concluded that topologies that contains series capacitor perform better for inductive load while shunt capacitor configuration gives good performance at high speeds prime mover; on the other hand the single capacitor configuration is only acceptable for resistive load. To enhance the power generation and power quality of the TWSPSEIG the authors in [15] presented a leaky minimal disturbance theory -based decoupled voltage and frequency controller. In [16] the author used fuzzy logic and practical approach to calculate the optimal capacitor for maximum output power of the SWSPSEIG.

Many research studies are carried out to maintain the voltage and frequency of the SPSEIGs constants under the variations of different operating conditions such as the prime mover speed and load dynamics. The most popular way to control voltage and frequency is using electronic load controller. In [17-19] a dummy load is used to compensate the fluctuation of the consumer load by controlling the power of that dump load. Another popular way to control voltage is using thyristor switched capacitor scheme to vary the reactive power supply [20-21]. In [22] the authors used a single-phase PWM inverter controlled by a microprocessor to adjust the output frequency of the TWSPSEIG driven by a variable speed prime-mover, while the excitation capacitor group is controlled by the microprocessor to keep the output voltage of the generator constant at variable operating conditions. In [23] the authors proposed a voltage source converter connected to a battery energy storage system at its DC bus. The system is controlled by an intelligent neural network-based control algorithm to maintain system voltage and frequency constant at all loading conditions. In [24] the authors proposed a combined control system that includes a dummy load and a secondary voltage control system, by adjusting the excitation capacitor connected to the auxiliary winding, in order to maintain system voltage and frequency constant of the TWSPSEIG.

In this paper, the authors deal with a TWSPSEIG with an excitation capacitor "C_A" which is connected across the auxiliary winding and a compensation capacitor "C_M" that is shunted with the load across the main winding. The performance equations at steady-state conditions are obtained by applying loop impedance method through the exact equivalent circuit models of the TWSPSEIG based on the double revolving field theory. The real and imaginary parts of the complex impedance of the equivalent circuits are rearranged to get two second order equations keeping

the values of the two capacitors C_A and C_M as unknowns for given values of generator parameters, prime mover speed, output frequency and load impedance. The two second order equations are then solved using simple iterative method to calculate the optimum values of the two capacitors under the constrains that the load voltage and frequency are constant at rated values irrespective the no load or different load conditions (different load impedance and power factor). The ranges of variation in the capacitors size to maintain constant load voltage and frequency while supplying variable load at variable prime mover speed are calculated. The steady-state results are confirmed by developing a dynamic model of the TWSPSEIG incorporating various no-load and load conditions and its nonlinearity behavior. The dynamic behavior of the TWSPSEIG at different operating conditions proves the capabilities of the proposed configuration and calculations method to maintain both the load voltage and frequency constants.

2. The Steady-state Model of TWSPSEIG

The basic scheme of the TWSPSEIG is shown in Fig.1. The equivalent circuits used for the steady-state analysis of the TWSPSEIG are shown in Fig.2. The steady-state equivalent circuits are based on the double revolving field theory under the assumptions that, neglecting the core loss and all the parameters of the generator, except the magnetizing reactances, are considered as constant and unaffected by saturation.

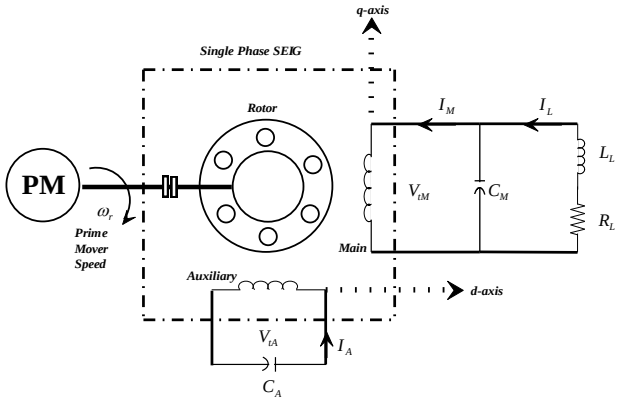

Fig.1 The basic scheme of TWSPSEIG

2.1 No-Load Model

At no-load the loop equations for the main and auxiliary currents can be written as:

$$Z_O * I_S = 0 \quad (1)$$

Where:

$$I_S = \begin{bmatrix} I_M \\ I_A \end{bmatrix} \quad (2)$$

$$Z_O = \begin{bmatrix} (Z_M - \frac{jX_{CM}}{a^2}) & \frac{jZ_{FBA}}{t} \\ -jtZ_{FBM} & (Z_A - \frac{jX_{CA}}{a^2}) \end{bmatrix} \quad (3)$$

$$Z_{1M} = \frac{R_{1M}}{a} + jX_{1M}$$

$$Z_{1A} = \frac{R_{1A}}{a} + jX_{1A}$$

$$Z_{FM} = \frac{\left[\frac{R_2}{(2(a-b))} + j\frac{X_2}{2}\right] * [j\frac{X_{mag}}{2}]}{\frac{R_2}{(2(a-b))} + j\frac{X_2}{2} + j\frac{X_{mag}}{2}}$$

$$Z_{BM} = \frac{\left[\frac{R_2}{(2(a+b))} + j\frac{X_2}{2}\right] * [j\frac{X_{mag}}{2}]}{\frac{R_2}{(2(a+b))} + j\frac{X_2}{2} + j\frac{X_{mag}}{2}}$$

$$Z_{FA} = \frac{\left[\frac{R_{2A}}{(2(a-b))} + j\frac{X_{2A}}{2}\right] * [j\frac{X_{magA}}{2}]}{\frac{R_{2A}}{(2(a-b))} + j\frac{X_{2A}}{2} + j\frac{X_{magA}}{2}}$$

$$Z_{BA} = \frac{\left[\frac{R_{2A}}{(2(a+b))} + j\frac{X_{2A}}{2}\right] * [j\frac{X_{magA}}{2}]}{\frac{R_{2A}}{(2(a+b))} + j\frac{X_{2A}}{2} + j\frac{X_{magA}}{2}}$$

$$Z_M = Z_{1M} + Z_{FM} + Z_{BM}$$

$$Z_A = Z_{1A} + Z_{FA} + Z_{BA}$$

$$Z_{FBM} = Z_{FM} - Z_{BM}$$

$$Z_{FBA} = Z_{FA} - Z_{BA}$$

From (1) since for steady state

$I_S \neq 0$

Therefore,

$|Z_o| = 0$. (i.e. Z_o must be singular matrix).

This implies that both real and imaginary parts of the determinant of "Z_o" are individually equals to zero; this can be simplified to the following two nonlinear equations:

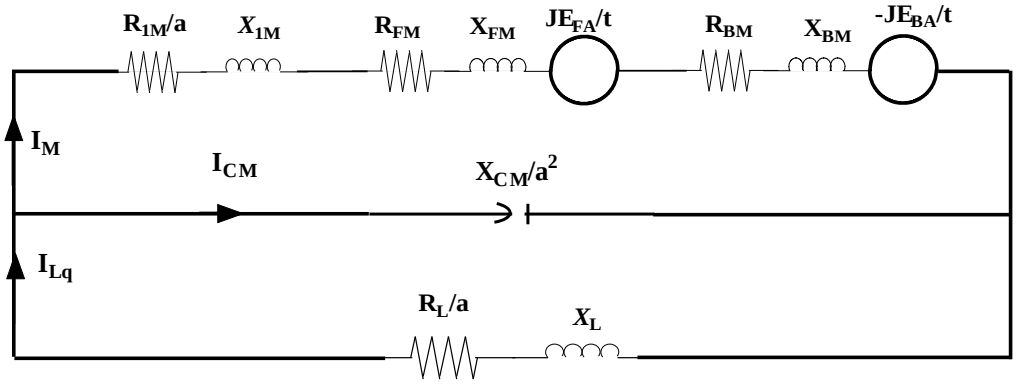

(a)

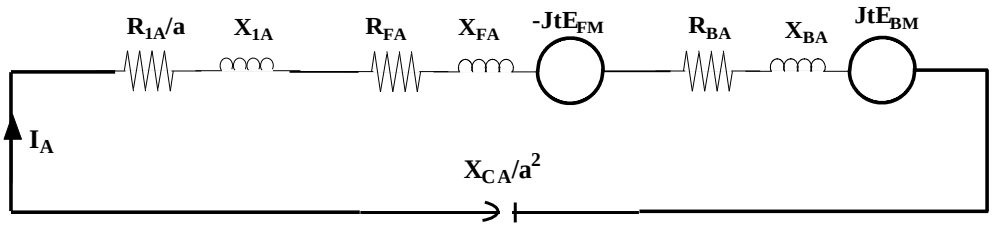

(b)

Fig.2 Steady-state equivalent circuits of a TWSPSEIG, (a) The main circuit, (b) The auxiliary circuit

The imaginary part yields:

$$A * X_{CM}^2 + B * X_{CM} + C = 0 \quad (4)$$

And the real part yields:

$$X_{CA} = \frac{1}{R_M} * (a^2 * (X_{MA} - X_{FBMA}) - R_A * X_{CM}) \quad (5)$$

Where:

$$A = \frac{R_A}{a^4 * R_M}$$

$$B = \frac{X_A}{a^2} + \frac{X_{FBMA}}{a^2 * R_M} - \frac{X_{MA}}{a^2 * R_M} - \frac{X_M * R_A}{a^2 * R_M}$$

$$C = R_{MA} + \frac{X_M}{R_M} * (X_{MA} - X_{FBMA}) - R_{FBMA}$$

$$Z_{FBMA} = Z_{FBM} * Z_{FBA} = R_{FBMA} + jX_{FBMA}$$

$$Z_{MA} = Z_M * Z_A = R_{MA} + jX_{MA}$$

The saturation portions of the magnetizing reactances of the main and the auxiliary circuits against the air-gap voltages (V_g &V_{gA}) could be piecewise linearized and expressed mathematically in the form:

$$X_{mag} = K_1 - K_2 * (\frac{V_g}{a}) \quad (6)$$

$$X_{magA} = K_3 - K_4 * (\frac{V_{gA}}{a}) \quad (7)$$

Where: K_1, K_2, K_3 and K_4 are constants.

Based on the analytical technique explained above, the required set values of the p.u. speed "b", the excitation capacitor "C_A" and the compensation capacitor "C_M" respectively, to achieve self-excitation at specified values of the no-load main terminal voltage and the p.u. frequency "a", could be computed as shown in the flowchart of Fig.(3).

2.2 Inductive Load Model

In this section a direct and simple method to predict the required values of main and auxiliary capacitances, under general inductive-load conditions, is developed to achieve the desired values of load voltage and frequency.

The loop equations for the currents (I_M, I_A and I_L) can be written as:

$$Z * I_S = 0 \quad (8)$$

Where:

$$I_S = \begin{bmatrix} I_M \\ I_A \\ I_L \end{bmatrix} \quad (9)$$

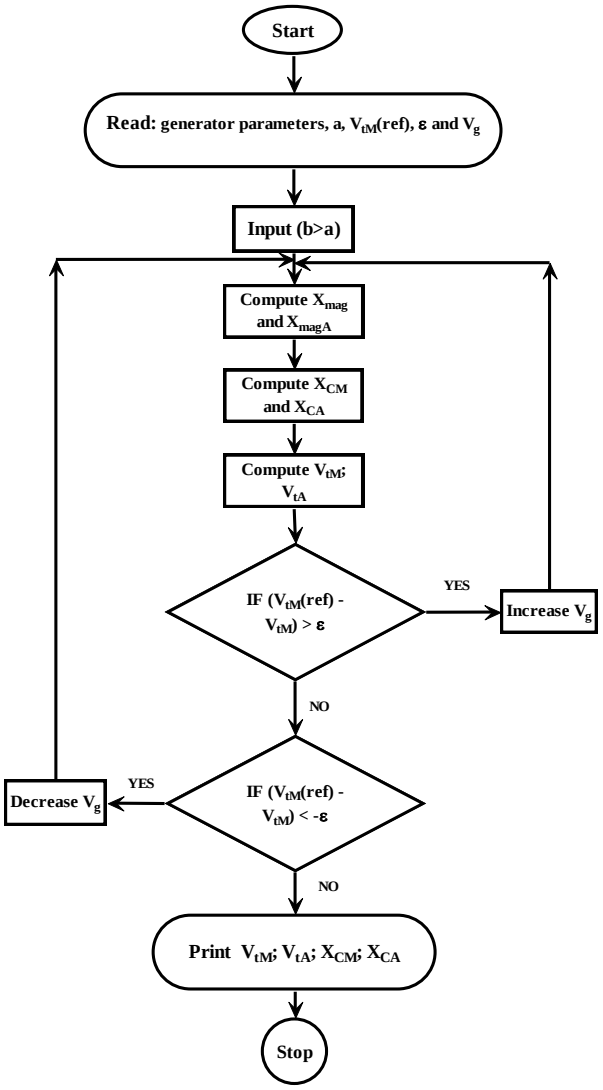

Fig.3. The flowchart of no-load computer algorithm

$$Z=\begin{bmatrix} (Z_M-\frac{jX_{CM}}{a^2}) & \frac{jZ_{FBA}}{t} & \frac{jX_{CM}}{a^2} \\ -jtZ_{FBM} & (Z_A-\frac{jX_{CA}}{a^2}) & 0 \\ \frac{jX_{CM}}{a^2} & 0 & (Z_L-\frac{jX_{CM}}{a^2}) \end{bmatrix} \quad (10)$$

Where:

$Z_L=\frac{R_L}{a}+jX_L$

From (8) since under steady state

$I_S \neq 0$

Therefore,

$|Z|=0$. (i.e. Z must be a singular matrix).

This implies that both real and imaginary parts of the determinant of "Z" must be equal to zero; this could be simplified to the following two nonlinear equations:
The imaginary part yields:

$$AA*X_{CM}^2+BB*X_{CM}+CC=0 \quad (11)$$

And the real part yields:

$$X_{CA}=\frac{A_1+A_2*(\frac{X_{CM}}{a^2})}{A_3*(\frac{X_{CM}}{a^4})-\frac{X_{ML}}{a^2}} \quad (12)$$

Where:

$AA=\frac{A_3*B_2-A_2*B_3}{a^6}$

$BB=\frac{A_3*B_1}{a^4}-\frac{B_2*C_1}{a^2}-\frac{A_2*C_2}{a^2}-\frac{A_1*B_3}{a^4}$

$CC=-B_1*C_1-A_1*C_2$

$A_1=R_{MAL}-R_{FBMAL}$

$A_2=X_{AL}+X_{MA}-X_{FBMA}$

$A_3=R_M+R_L$

$B_1=X_{MAL}-X_{FBMAL}$

$B_2=R_{FBMA}-R_{MA}-R_{AL}$

$B_3=X_M+X_L$

$C_1=\frac{X_{ML}}{a^2}$, $C_2=\frac{R_{ML}}{a^2}$

$Z_{FBMAL}=Z_{FBM}*Z_{FBA}*Z_L=R_{FBMAL}+jX_{FBMAL}$

$Z_{MAL}=Z_M*Z_A*Z_L=R_{MAL}+jX_{MAL}$

$Z_{AL}=Z_A*Z_L=R_{AL}+jX_{AL}$

Based on the analytical technique explained above, the required set values of the p.u. speed "b", the excitation capacitor "C_A" and the compensation capacitor "C_M" respectively, to achieve the specified values of the load voltage and the operating p.u. frequency (a), at a general load impedance (Z_L) could be computed as shown in the flowchart of Fig.(4).

3. Dynamic Model of the TWSPSEIG

Generally the induction machine models are developed using simplified model in q-d reference frame attached to stator, rotor or synchronous rotating reference. In this work a q-d reference frame attached to stator as shown in Fig.1 is used to develop the dynamic model of the TWSPSEIG. The voltage differential equations in the q-d reference frame can be represented as:

$$\begin{bmatrix} V_{qs} \\ V_{ds} \\ V_{qr} \\ V_{dr} \end{bmatrix} = \begin{bmatrix} R_{1M} + pL_{1M} & 0 & pl_{mag} & 0 \\ 0 & R_{1A} + pL_{1A} & 0 & pl_{magA} \\ pl_{mag} & \frac{-\omega_r l_{magA}}{t} & R_2 + pL_2 & \frac{-\omega_r L_{2A}}{t} \\ \omega_r l_{mag} t & pl_{magA} & \omega_r L_2 t & R_{2A} + pL_{2A} \end{bmatrix} * \begin{bmatrix} I_{qs} \\ I_{ds} \\ I_{qr} \\ I_{dr} \end{bmatrix} \quad (13)$$

Where:

$L_{1M} = l_{1M} + l_{mag}$

$L_{1A} = l_{1A} + l_{magA}$

$L_2 = l_2 + l_{mag}$

$L_{2A} = l_{2A} + l_{magA}$

At no-load condition, the main and the auxiliary winding currents are equals to the currents in the q-d frame as in (14), the magnetization current components in the direct and quadrature axes are given in (15), and the magnitude of the magnetizing current is given in (16).

$$I_{qs} = I_M \qquad I_{ds} = I_A \quad (14)$$

$$I_{magq} = I_{qs} + I_{qr} \qquad I_{magd} = I_{ds} + I_{dr} \quad (15)$$

$$I_{mag} = \sqrt{\left({I_{magq}}^2 + {I_{magd}}^2 \right)} \Big/ \sqrt{2} \quad (16)$$

The generator terminal voltages (the voltages across the main and the auxiliary capacitor) as a function of the generator currents at no load condition are given by:

$$\begin{bmatrix} I_{qs} \\ I_{ds} \end{bmatrix} = \begin{bmatrix} -pC_M & 0 \\ 0 & -pC_A \end{bmatrix} * \begin{bmatrix} V_{qs} \\ V_{ds} \end{bmatrix} \quad (17)$$

At load condition the TWSPSEIG will be loaded with a load connected to the generator terminals across the main winding (compensation) capacitor "C_M". To develop the generator dynamic model considering the load, the q-d components of the stator currents have to be computed as in (18).

$$I_{qs} = I_{C_M} + I_{Lq} \qquad I_{ds} = I_{C_A} = I_A \quad (18)$$

The generator terminal voltages (V_{qs}, V_{ds}) as a function of the generator currents (I_{qs}, I_{ds}) and the load current (I_{Lq}) at load condition is given by:

$$\begin{bmatrix} I_{qs} \\ I_{ds} \\ I_{Lq} \end{bmatrix} = \begin{bmatrix} -pC_M & 0 & 1 \\ 0 & -pC_A & 0 \\ -1/R_L & 0 & -pL_L/R_L \end{bmatrix} * \begin{bmatrix} V_{qs} \\ V_{ds} \\ I_{Lq} \end{bmatrix} \quad (19)$$

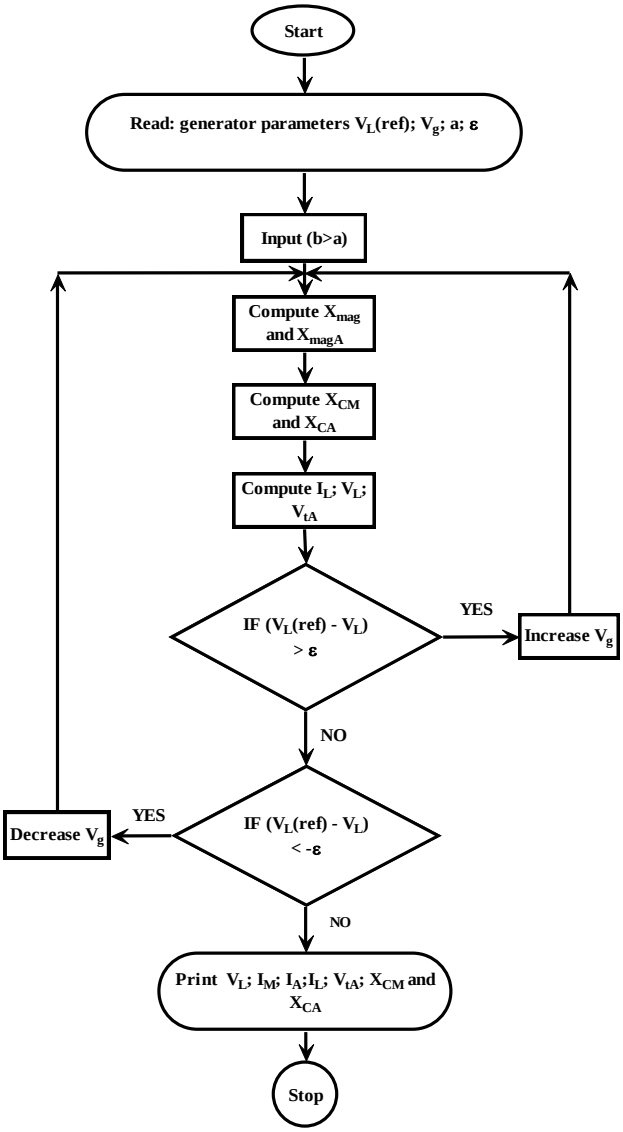

Fig.4. The flowchart of load computer algorithm

4. Simulation Results

The performance characteristics of 0.75 kW, 230 V, 6 A, 4-poles and 50Hz single phase induction generator are carried out via the proposed technique. Table 1 gives the parameters of the generator. The magnetization characteristics of the TWSPSEIG are shown in Fig.5. Results for steady-state and dynamic simulations are provided in this section.

Table 1 Equivalent circuit parameters of the TWSPSEIG

R_{1M}	3.41 ohm
R_{1A}	11.22 ohm
R_2	4.37 ohm
R_{2A}	8.01 ohm
X_2	3.99 ohm
X_{2A}	6.433 ohm
X_{1M}	3.99 ohm
X_{1A}	6.433 ohm
t	1.4

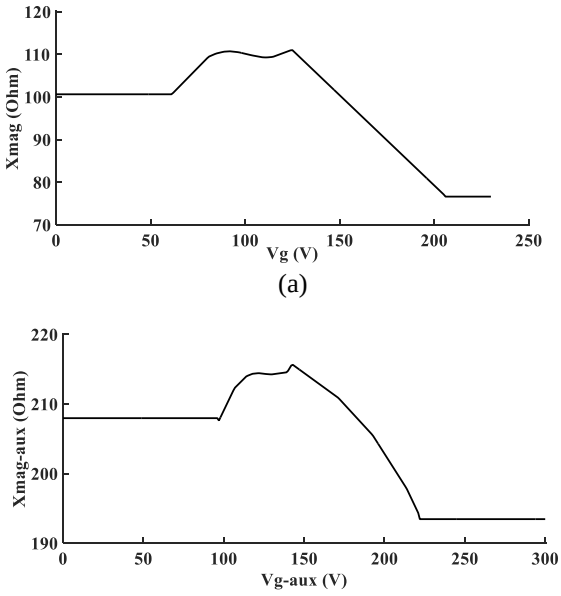

Fig.5 The magnetization characteristic for (a) main winding and (b) auxiliary winding

4.1. Steady-state Simulation Results

In steady-state, a MATLAB program was used to estimate the values of the main and the auxiliary windings capacitors. The relation between the speed and the values of capacitors under the variation of the load and its power factor will be presented.

Fig.6 shows the required capacitances for self excitation versus the P.U. speed at constant rated terminal voltage and frequency at no load conditions.

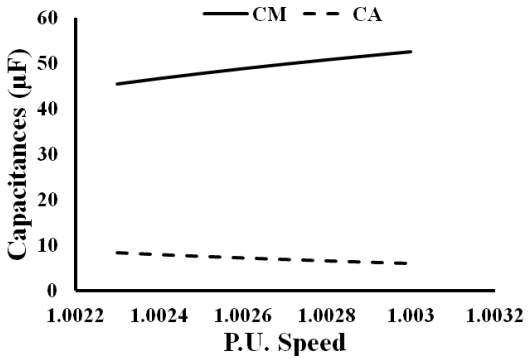

Fig.6 Main and Auxiliary capacitance versus P.U. speed at rated voltage and frequency

Fig.7 shows the variation of the P.U. speed limits versus the terminal voltage to maintain the operating frequency, under no load, constant at the rated value. It may be noted that, the maximum speed is almost constant with the increase of the terminal voltage.

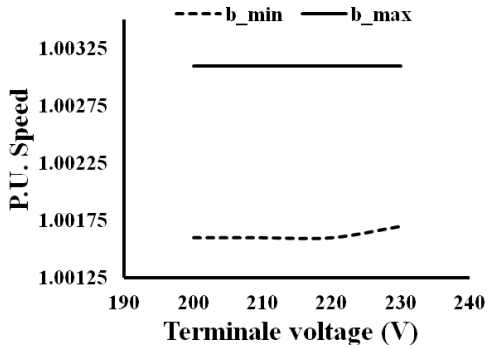

Fig.7 P.U. speed versus no-load terminal voltage at rated frequency

If the generator is driven by unregulated prime-mover, then it is necessary to continuously vary the capacitors to cope with changing of the operating conditions. Under such condition it is necessary to investigate the speed limits between which the generator is capable to build up constant rated load terminals voltage and frequency for different loads. Fig.8 shows the variation of the P.U. speed limits for resistive loads, while Fig.9 shows the variation of the P.U. speed limits for inductive loads with a power factor of 0.97.

To maintain the rated load voltage and frequency for any speed within the speed limits, the set of capacitors (main and auxiliary capacitors) will be calculated using the proposed technique. Figs.10:12 give the required values of the main and the auxiliary capacitances versus the operating speed at different loads.

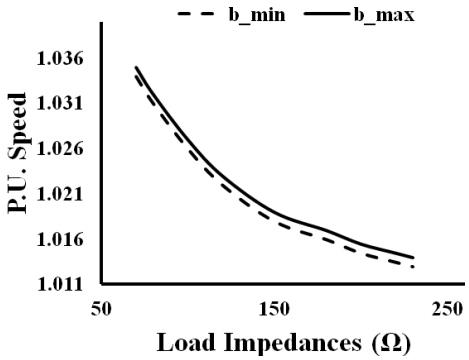

Fig.8 Limits of P.U. speed versus load impedances at rated load terminals voltage and frequency for resistive loads

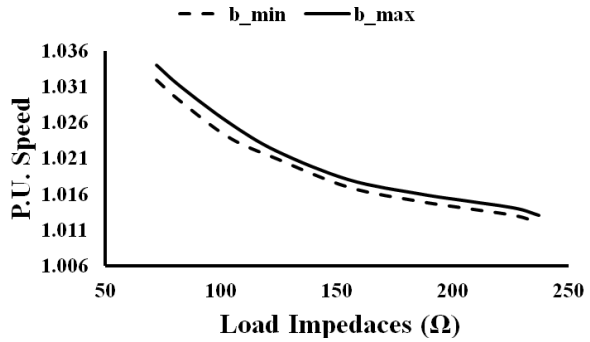

Fig.9 Limits of P.U. speed versus load impedances with 0.97 power factor at rated load terminals voltage and frequency.

It is observed that the main capacitance increases and the auxiliary capacitance decreases as the speed increases in all cases. Also it can be concluded from these figures that the speed limits increases as the load power factor increases.

4.2. Dynamic Simulation Results

For the dynamic simulation, a MATLAB program was developed to demonstrate the dynamic response of different voltages and currents building up processes of the studied TWSPSEIG under no-load and load conditions.

Fig.13 shows the dynamic response of the TWSPSEIG during self-excitation under no-load condition. The generator initially runs at a P.U. speed of 1.0025 (1504 rpm) with a 47.838 µF main capacitance and a7.5786 µF auxiliary capacitance. The corresponding stator currents are also included in Fig.13 (c,d) and they closely resemble the voltages waveforms. Fig.13 (e,f) also show the variation of magnetizing inductances during the voltage building up process and Fig.13 (g) shows the frequency of the main winding voltage.

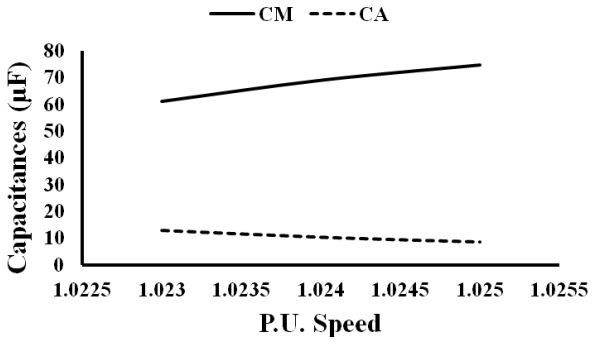

Fig.10 Main and Auxiliary capacitance versus P.U. speed at a load of 95 ohm and 0.85 power factor

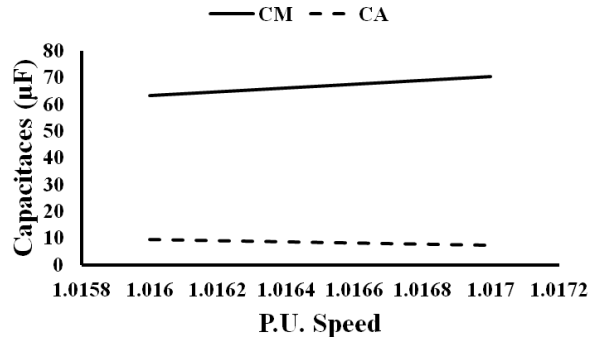

Fig.11 Main and Auxiliary capacitance versus P.U. speed at a load of 135 ohm and 0.75 power factor

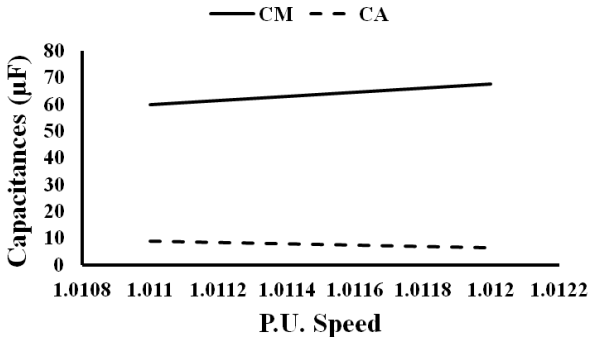

Fig.12 Main and Auxiliary capacitance versus P.U. speed at a load of 185 ohm and 0.65 power factor

Fig.14 shows the dynamic response of the studied no-load TWSPSEIG subjected to a sudden connection of a resistive load of 100 ohm at time 5 sec. and a P.U. speed of 1.0026, with a 49.8 µF main capacitance and an 11.305 µF auxiliary capacitance. Sudden change of the P.U. speed to 1.0027 at time 6 sec., with the main capacitance of 53 µF and the auxiliary capacitance of 9.4825 µF.

Fig.15 shows the dynamic response of the studied no-load TWSPSEIG subjected to a sudden connection of an

inductive load of 125 ohm with 0.97 power factor at time 5 sec. and a P.U. speed of 1.0021, with the main capacitance of 54.9 µF and the auxiliary capacitance of 10.736 µF. Then sudden change of the P.U. speed to 1.0022 at time 6 sec. is applied, with the main capacitance of 58.5 µF and the auxiliary capacitance of 8.6148 µF.

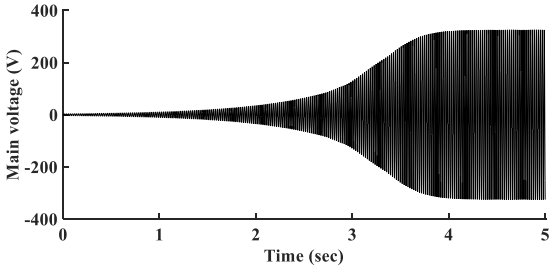

(a)

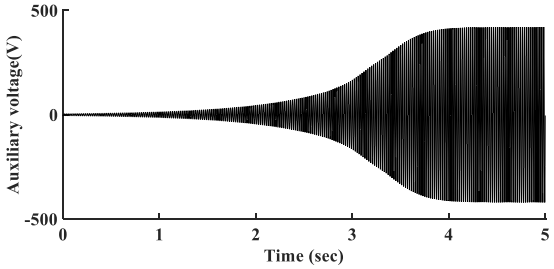

(b)

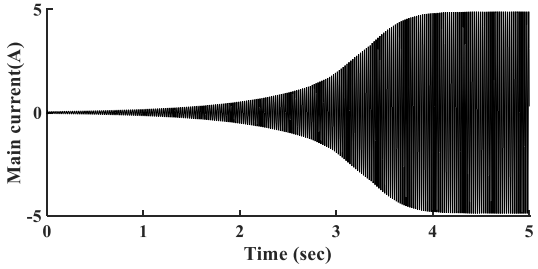

(c)

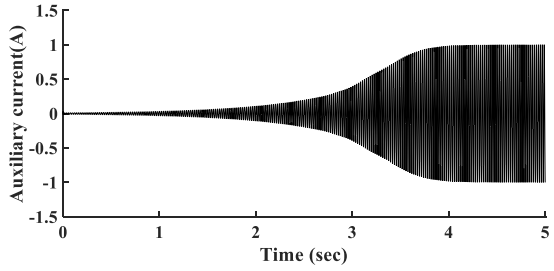

(d)

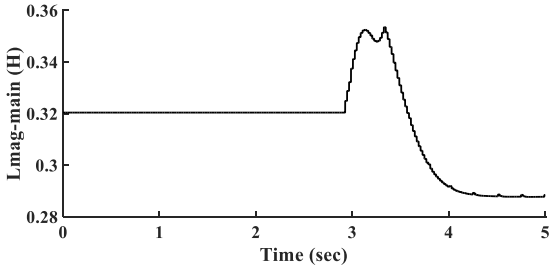

(e)

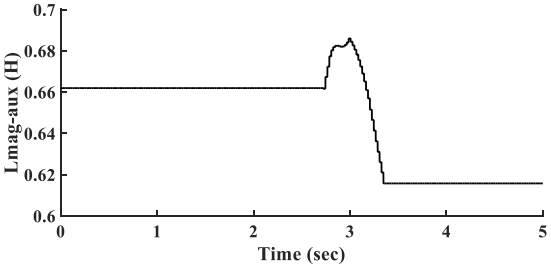

(f)

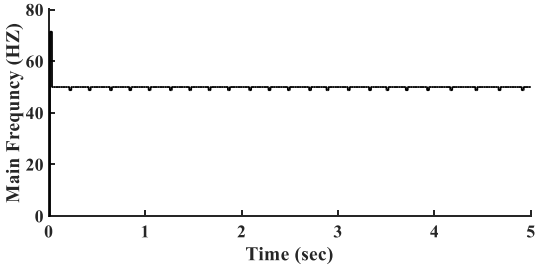

(g)

Fig.13 No-Load building up process (a) main winding voltage, (b) auxiliary winding voltage (c) main winding current, (d) auxiliary winding current (e) main winding magnetizing inductance, (f) auxiliary winding magnetizing inductance and (g) main winding frequency

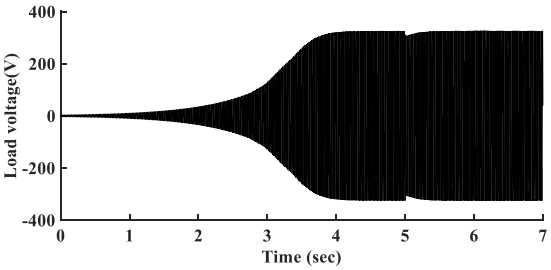

(a)

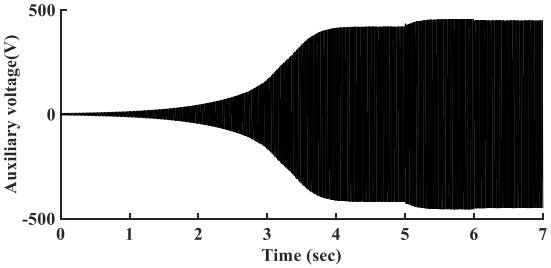

(b)

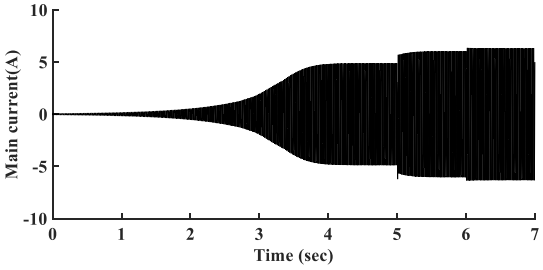

(c)

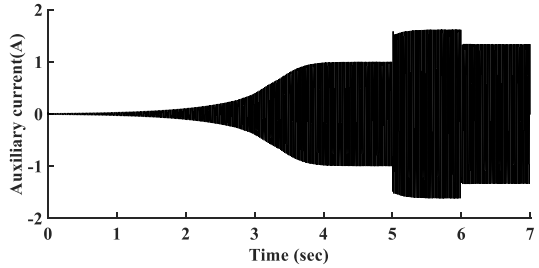

(d)

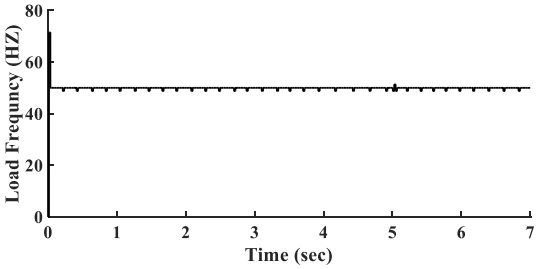

(e)

Fig.14 Dynamic responses of the TWSPSEIG at a resistive load (a) Load terminal voltage, (b) Auxiliary voltage, (c) Main current, (d) Auxiliary current and (e) Load frequency

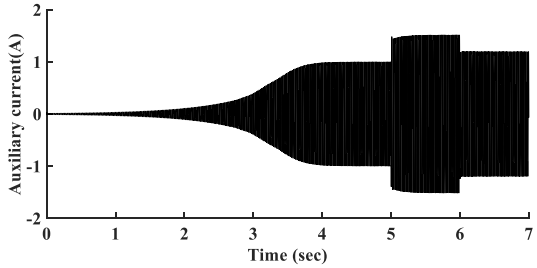

(d)

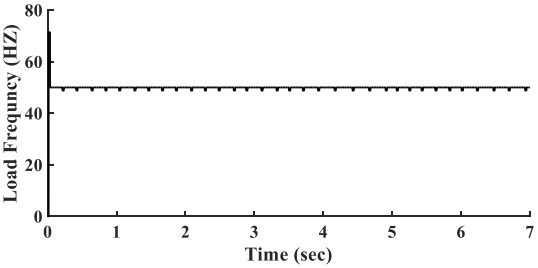

(e)

Fig.15 Dynamic responses of the TWSPSEIG at an inductive load (a) Load terminal voltage, (b) Auxiliary voltage, (c) Main current (d) Auxiliary current and (e) Load frequency

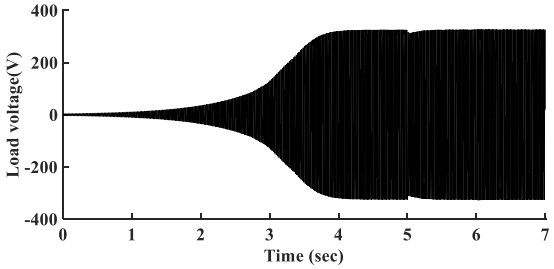

(a)

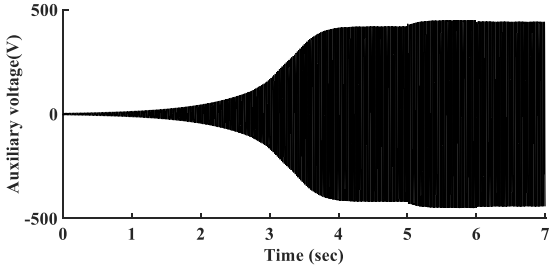

(b)

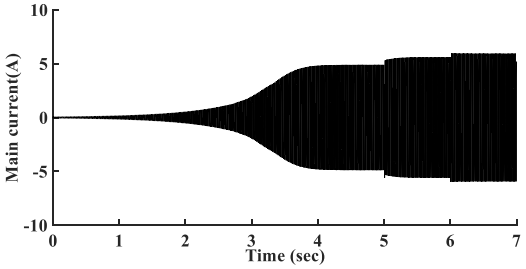

(c)

Figs.14&15 illustrate that the load voltage and frequency are almost constant at rated values regardless the values of load impedance, load power factor and operating speed, which is a proof of the validity and accuracy of the proposed technique for calculations of the suitable main and auxiliary capacitances.

Table 2 summaries different cases for the dynamic response of the TWSPSEIG operated at no load then subjected to a sudden connection of different resistive loads. Table 3 summaries different cases of the dynamic response of the TWSPSEIG operated at no load then subjected to a sudden connection of different inductive loads with different power factors. It is observed that the operating speed decreases as the load current decreases at constant power factor.

5. Conclusion

In this paper the two windings single phase self-excited induction generator (TWSPSEIG) has been studied in details and a suitable methodology has been developed. A new technique to analyze the steady-state behavior of the TWSPSEIG with unregulated prime mover is presented to maintain both of the terminal voltage and frequency at constant rated values. It is found that to maintain both of the terminal voltage and frequency at constant rated values there are ranges of the operating speed, which differs according to the values of load current and power factor. The required set values of

the main and auxiliary capacitors have been calculated at different load conditions and operating speed by using simple iterative technique. The paper also introduces a new simple and direct method for finding the minimum capacitance required for self-excitation at no-load conditions with the variation of the operating speed. To verify the steady-state results the paper introduces a dynamic model of the TWSPSEIG incorporating various no-load and load conditions and its nonlinearity behavior. The dynamic behavior of the TWSPSEIG at different operating conditions proves the capabilities of the proposed configuration and calculations method to maintain both the load voltage and frequency constants.

References

[1] Aleksander Leicht, Krzysztof Makowski: *A single-phase induction motor operating as a self-excited induction generator*. In: Archives of electrical engineering, Vol. 62, No.3, pp. 361-373, 2013.

[2] Faisal Khan, M., Rizwan Khan, M.: *Evaluation of Excitation Capacitance for a Single-Phase Two Winding Self-Excited Induction Generator*. In: Proceedings of IEEE International Conference on Power Electronics, Drives and Energy Systems (PEDES), Mumbai India, 16-19 December 2014, pp.1-6.

[3] Satnam Mahley, Sanjay Kumar Jain: *Optimal Operation of Single-Winding Self-Excited Induction Generator for Single-Phase Power Generation*. In: Proceedings of 7th International Conference on Power Electronics (IICPE), Patiala, India, 17-19 November 2016, pp. 1-5.

[4] Bhim Singh, Shilpakar, L. B., Murthy, S. S., Tiwari, A. K.: *Improved Steady-state and Transient Performance with Optimum Excitation of Single-Phase Self-Excited Induction Generator*. In: Electric Machines and Power Systems, Vol.28, pp. 591–604, 2000.

[5] Mohd. Alinasr Saif, Khan, B. H.: *A Simplified Analysis of a Constant Voltage Single Phase Self-Excited Induction Generator*. In: Electric Power Components and Systems, Vol.33, pp. 103–112, 2005.

[6] Faisal Khan, M., Rizwan Khan, M.: *Voltage control of Single-Phase Two Winding Self-Excited Induction Generator for isolated loads*. In: Proceedings of International Conference on Advances in Energy Conversion Technologies (ICAECT), 23 – 25 January 2014, Manipal, India, pp. 209-214.

[7] Ujjwal Kumar Kallla, Bhim Singh, Divya Jain: *A Study of Experimental Investigations on Two Winding Single-Phase Self-Excited Induction Generators*. In: Proceedings of IEEE IAS Joint Industrial and Commercial Power Systems / Petroleum and Chemical Industry Conference (ICPSPCIC), Hyderabad, India, 19-21 November 2015, pp. 45-51.

[8] Anagreh, Y.N.: *Matlab-Based Steady State Analysis of Single-Phase Self-Excited Induction Generator*. In: International Journal of Modeling and Simulation, Vol. 26, No. 3, pp. 271-275, 2006.

[9] Velusami, S., Singaravelu, S.: *Steady-state Modeling and Analysis of Single-phase Self-excited Induction Generators.* In: Electric Power Components and Systems, Vol.35, pp.63–79, 2007.

[10] Olorunfemi Ojo: *Performance of Self-Excited Single-Phase Induction Generators with Shunt, Short-Shunt and Long-Shunt Excitation Connections*. In: IEEE Transactions on Energy Conversion, Vol. 11, No. 3, pp. 477-482, 1996.

[11] Singh, B. and Shilpkar, L.B.: *Steady-state analysis of single-phase self-excited induction generator*. In: IEE Proc-Gener. Transm. Distrib., Vol. 146, No. 5, pp. 421-427, September 1999.

[12] Faisal Khan, M., Rizwan Khan, M., Atif Iqbal: *Performance Comparison of Single Winding and Double Winding Self-excited Induction Generators.* In: Proceedings of IEEE Conference on Clean Energy and Technology (CEAT), 18 - 20 November 2013, Langkawi, Malaysia, pp.202-207.

[13] Velusami, S., Singaravelu, S.: *Steady-state modeling and fuzzy logic based analysis of wind driven single phase induction generators*. In: Renewable Energy, Vol. 32, pp.2386–2406, 2007.

[14] Satnam Mahley, Sanjay Kumar Jain: *Investigations on Single-Phase Two Winding Self-Excited Induction Generator for Optimal Operation with Different Capacitor Topologies*. In: Proceedings of 7th International Conference on Power Electronics (IICPE), Patiala, India, 17-19 November 2016, pp.1-6.

[15] Ujjwal Kumar Kalla, Bhim Singh, and Sreenivasa Murthy, S.: *Enhanced Power Generation From Two-Winding Single-Phase SEIG Using LMDT-Based Decoupled Voltage and Frequency Control.* In: IEEE Transactions on Industrial Electronics, Vol. 62, No. 11, pp.6934-6943, November 2015.

[16] Senthilkumar, M.: *Optimal Capacitor for Maximum Output Power Tracking Of Self Excited Induction Generator Using Fuzzy Logic Approach*.

In: International Journal on Computer Science and Engineering Vol. 02, No. 05, pp. 1758-1762, 2010.

[17] Dheeraj Kumar Palwalia and Singh, S. P.: *DSP Based Induction Generator Controller for Single Phase Self Excited Induction Generator*. In: International Journal of Emerging Electric Power Systems, Vol. 9, No.1, Article 2, pp.1-9, 2008.

[18] Ahshan, R. and Iqbal, M.T.: *Voltage Controller of a Single Phase Self-Excited Induction Generator*. In: The Open Renewable Energy Journal, Vol. 2, pp.84-90, 2009.

[19] Ujjwal Kumar Kalla, Bhim Singh, and Sreenivasa Murthy, S.: *Modified Electronic Load Controller for Constant Frequency Operation With Voltage Regulation of Small Hydro-Driven Single-Phase SEIG*. In: IEEE Transactions on Industry Applications, Vol. 52, No. 4, pp. 2789-2800, July/August 2016.

[20] Murthy, S. S., Ujjwal Kumar Kalla, Bhuvaneswari, G.: *A Novel Electronic Controller Implementation for Voltage Regulation of Single Phase Self-Excited Induction Generator*. In: Proceedings of 2010 IEEE Industry Applications Society Annual Meeting (IAS), Houston, TX, USA, 3-7 October 2010, pp.1-8.

[21] Ujjwal Kumar Kalla, Bhim Singh, and Murthy, S. S.: *Implementation of Voltage Controller of Single-phase Self-excited Induction Generator*. In: Electric Power Components and Systems, Vol.44, pp.1276–1290, 2016.

[22] Ünal, S., Özdemir, M., Sünter, S.: *Voltage and Frequency Control of a Single-Phase Self-Excited Asynchronous Generator*. In: Proceedings of International Aegean Conference on Electrical Machines and Power Electronics (ACEMP), İstanbul, Turkey, May 2004, pp.509-514.

[23] Ujjwal Kumar Kalla, Bhim Singh, and Murthy, S. S.: *Intelligent Neural Network-Based Controller for Single-Phase Wind Energy Conversion System Using Two Winding Self-Excited Induction Generator*. In: IEEE Transactions on Industrial Informatics, Vol. 12, No. 6, pp.1986-1997, December 2016.

[24] Widodo Pudji Muljanto, Rinaldy Dalimi: *Secondary Voltage Control of Single Phase Induction Generator Operated In Small Scale Picohydro Power Plant At Off-Grid Area*. In: Proceedings of 15th International Conference on Quality in Research (QiR): International Symposium on Electrical and Computer Engineering, 24-27 July 2017, Nusa Dua, Indonesia, pp.303-308.

Table 2 Dynamic responses of the TWSPSEIG at resistive loads

Load (Ω)	P.U. speed	C_M (μF)	C_A (μF)	V_A (V)	I_M (A)	I_A (A)	I_L (A)
70	1.034	46	15.906	341.9348	4.6810	1.7043	3.2891
80	1.031	48.8	13.406	332.8854	4.5674	1.3990	2.8833
120	1.022	48.3	11.22	320.7460	3.9997	1.1289	1.9228
150	1.018	46.7	11.209	317.1514	3.7119	1.1152	1.5336
180	1.016	49.3	9.1121	310.4355	3.7955	0.8880	1.2798
200	1.0145	48.3	9.4465	310.4145	3.6852	0.9204	1.1519
220	1.0135	48.6	9.0737	309.4222	3.6828	0.8814	1.0495
230	1.013	48.4	9.0962	309.0380	3.6544	0.8825	1.0035

Table 3 Dynamic responses of the TWSPSEIG at inductive loads

Load (Ω)	P. F.	P.U. speed	C_M (μF)	C_A (μF)	V_A (V)	I_M (A)	I_A (A)	I_L (A)
72	0.97	1.032	54.2	16.559	343.0854	4.4443	1.7802	3.2008
105	0.97	1.024	54	12.797	326.0599	4.0080	1.3084	2.2
155	0.97	1.017	51.5	11.181	316.8536	3.6625	1.1113	1.4880
185	0.97	1.015	52.3	9.6382	310.8737	3.6863	0.9404	1.2394
205	0.97	1.014	52.9	8.7949	308.7676	3.7296	0.8526	1.122
235	0.97	1.012	49.7	10.153	310.7980	3.4974	0.9902	0.979
95	0.85	1.023	63.9	12.842	325.5212	3.9256	1.3109	2.4212
135	0.75	1.016	64.3	9.6482	312.1127	3.7503	0.9451	1.704
185	0.65	1.011	61	8.9844	306.5125	3.5597	0.8646	1.244